SAND2019-13965B

MNL20-2ND-EB/Jan. 2005

18

# Pitting

*Robert G. Kelly[1], Ryan M. Katona[2,3], Eric J. Schindelholz[3]*

## INTRODUCTION

PITTING CORROSION occurs when discrete areas of a material undergo rapid attack, although the vast majority of the surface remains virtually unaffected. This morphology is in sharp contrast to uniform corrosion in which all parts of the exposed surface recede at approximately the same rate. Essentially, all metals and alloys undergo pitting corrosion under some set of experimental conditions, although the relative susceptibility varies widely. The basic requirement for pitting is the existence of a passive state for the material in the environment of interest. Pitting occurs when portions of the metal surface lose their passivity and dissolve rapidly. This loss of passivity often occurs at heterogeneities in the surface (either physical or chemical). Pitting of a given material depends strongly on the presence of an aggressive species in the environment and a sufficiently oxidizing potential (e.g., $Cl^-$ ion in neutral, aerated aqueous solution for Type 304 stainless steel). There are many metal/environment combinations that can lead to pitting, as extensively reviewed by Szlarska-Smialowska [1] and Frankel [2] and more recently by Soltis [3]. In many situations, pitting can severely limit the performance of the material.

Testing for localized corrosion resistance usually aims at meeting one (or more) of four general goals: (a) alloy ranking for selection or development; (b) failure analysis; (c) determination of the effects of changes in process parameters; and (d) prediction of penetration rates. Of the four, the last is by far the most difficult to accomplish, but also the most important in many cases. This chapter discusses the different types of tests that have been developed for pitting corrosion. The physical and chemical basis for each test is described, as are some of the practical applications and limitations. The first section describes coupon exposure testing, while the second describes electrochemical testing.

### COUPON TESTING

The exposure of test coupons to corrosive solutions to evaluate localized corrosion resistance has a long and successful history. The materials of interest are typically machined into coupon form before being measured, cleaned, weighed, and exposed to the corrosive medium. After a set period of time, the coupons are removed; the surfaces are carefully cleaned and evaluated for attack. General requirements and information on coupon testing can be found elsewhere in this manual as well as in other sources [4,5] . ASTM G 1, Practice for Preparing, Cleaning, and Evaluating Corrosion Test Specimens, describes the details of the preparation of test coupons. ASTM G 4, Standard Guide for Conducting Corrosion Tests in Field Applications, details related information on the performance of such tests in plant equipment under operating conditions. The advantages of properly conducted coupon testing include the fact that actual process streams can be used, a large number of coupons can be exposed simultaneously, and various forms of corrosion can be detected. Disadvantages include the inability to monitor the time dependence of the corrosion process and the long exposure times usually required to characterize both the initiation period and the propagation rate.

#### Coupon Preparation and Analyses

Because detailed information on coupon testing is available elsewhere, this section will focus on the aspects of such testing that are specific to the evaluation of pitting corrosion. When performing coupon exposures, it is important to include alloys whose corrosion behavior in the environment of interest is well characterized and reproducible to serve as an internal standard. This protocol is of particular importance when localized corrosion is studied. Because pitting has a stochastic nature, the use of these "controls" increases the confidence with which final material selection choices are made. If the control materials behave as expected, it is probable that the results for the other materials reflect typical behavior for the environment of interest.

Whereas mass loss characterizes the rate of uniform corrosion well, such measurements can be extremely misleading for pitting

[1]AT&T Professor of Engineering, Department of Materials Science and Engineering, University of Virginia, P.O. Box 400745, 295 McCormick Rd, Charlottesville, VA 22904.
[2]Department of Materials Science and Engineering, University of Virginia, Charlottesville, VA, 22904
[3]Sandia National Laboratories, Albuquerque, New Mexico 87123, USA

corrosion. Badly pitted specimens can exhibit negligible weight loss if the attack is extremely localized. In fact, the more a given amount of attack is localized, the more severe the pitting problem. ASTM G 46, Practice for the Examination and Evaluation of Pitting Corrosion, describes different methodologies for evaluating pitting corrosion attack. Visual attack of both cross sections and plane views of pitted specimens can be ranked as shown in the standard. Whereas pit density (number/$cm^2$) is important, pit depth measurement is often the most directly applicable measurement [6]. Values for both average pit size and for the deepest pit observed are useful. To quantitatively evaluate the depth of attack, a variety of measurement methods can be used including depth gages, metallographic examination of cross sections, or change in the focus plane on a metallurgical microscope, depending on the size of the pits. Direct measurement of pit depth using optical profilometry is attractive in that pit depths and distributions can be obtained rapidly. All line-of-sight methods are unable to detect and characterize undercutting pits (i.e., those with "ink-bottle" shapes or those with lacy covers [7]).The pitting factor (PF) is the ratio of the average of the ten deepest observed pits to the average metal penetration by uniform dissolution, with higher values indicating a greater susceptibility to pitting. Statistical methods have also been applied to the evaluation of pitting corrosion (see ASTM G 16, Guide for Applying Statistics to Analyses of Corrosion Data, and Refs [8] and [9]). In terms of predictive capability, the use of extreme value statistics is attractive [9]. Plotting the measured maximum pit depths for a large number of small samples has been used to estimate the probability that a pit of a specific depth will occur under the same conditions for a larger area.

**Exposure Environments**

There are two general types of environments used in coupon testing for pitting corrosion: those that simulate service conditions and those that seek to accelerate the pitting process. Tests in simulated (or actual) service environments are extremely valuable due to their direct applicability [10,11]. However, because time is often of the essence, the long exposure times required usually limit the use of such tests to (a) confirmation of decisions made on the basis of accelerated laboratory tests, and (b) corrosion monitoring. The aim of testing in accelerating environments is usually alloy ranking or screening. Thus, little information is gained on the expected rate of attack in the actual application. However, the relative susceptibility of different alloy compositions or the effects of heat treatments, welding, or other processing can be assessed rapidly and quantitatively.

There is a variety of accelerated exposure tests that have been developed to aid engineers in material selection for corrosion resistance. This section will review some of those that are useful for localized corrosion resistance. Besides a brief description of the test, the scientific reasoning behind it is presented, along with comments concerning the limits of its applicability, and alterations one can make to improve the utility of the test for a specific application. An experimenter should not feel bound by the structures of the ASTM standards if he or she can justify that by changing the procedure, more relevant information can be gained. However, it should be noted that these ASTM tests are probably the most widely used tests for localized corrosion resistance. Thus, an understanding of them can be of great importance in analyzing the results of testing performed in other labs or by manufacturers.

*ASTM G 48, Test Method for Pitting and Crevice Corrosion Resistance of Stainless Steels and Related Alloys by the Use of Ferric Chloride Solution*

This test involves exposure of the material to a highly oxidizing, highly acidic, concentrated metal chloride solution. In essence, it is an attempt to simulate very roughly the composition of the environment within a localized corrosion site in a stainless steel. Briefly, a material is exposed to a 10 wt% $FeCl_3$ solution for a relatively short time (24-72 h) at either ambient or elevated (usually 50°C) temperature. At the end of the test, the sample is examined for weight loss and localized attack (see ASTM G 46 for a recommended practice for evaluating the extent of pitting corrosion). If pitting and crevice corrosion are of concern, artificial crevices can be applied by the use of Teflon® blocks held tightly to the sample surface by rubber bands (see ASTM G 48). Ferric chloride exposure is commonly used for assessing the corrosion resistance of stainless steel weldments (typically per ASTM G 48, method A).

The basic concept behind this test is the application of a high potential using a chemical potentiostat in an acidic, concentrated chloride solution. The ferric salt forms a $Fe^{3+}/Fe^{2+}$ redox couple with a potential of approximately +0.45 V(SCE). The high concentration of ferric ion allows the couple to provide a large current without an appreciable change in potential (approaching an ideally nonpolarizable electrode). The cathodic reaction (reduction of ferric to ferrous ion) occurs on the boldly exposed passive surface of the material under test. Thus, the redox couple serves the role of the *chemical* potentiostat. The high potential in turn nearly guarantees that the pitting potential will be exceeded, especially in such a concentrated $Cl^-$ solution (and even more so if the test temperature is raised to 50°C). The low pH of the solution (typically about 1.3) inhibits repassivation and lowers the stability of the passive film. Thus, the ferric chloride test is a test of the resistance of an alloy to propagation of localized corrosion for most alloys, because their pitting potentials are well below +0.45 V(SCE). However, more highly alloyed materials can resist initiation in this solution, and thus the time of the test can be extended to a period of many days or the temperature increased.

This very popular test does have a number of limitations. Very few industries operate in 10 wt% $FeCl_3$. Thus, the relation of the results of this test to material performance in real service environments that are profoundly different is questionable, and in fact, reversals in alloy ranking can occur. For nickel-base materials, the use of a ferric ion solution is also of questionable value. Despite these limitations, the $FeCl_3$ test will continue to be an important tool in alloy development and screening for historical, if for no other reasons.

The ferric chloride test details can be modified and still fall within the spirit of the requirements of the published method. The

exposure time and temperature can be altered, as can the surface finish. As mentioned above, surface finish can have important impact on the localized corrosion behavior. For example, it can affect the geometry of occluded sites and, in some cases, it can alter the surface area for cathodic reactions. Thus, it is important that the surface finish be chosen with care to simulate the expected conditions of the application.

*B 117 Standard Practice for Operating Salt Spray (Fog) Apparatus and G 85 Standard Practice for Modified Salt Spray (Fog) Testing*

Probably the most widely used test for pitting resistance is salt spray. B 117 describes the experimental arrangements to be used and mandates the use of 5 wt.% NaCl at slightly elevated temperature (35°C). The test chamber allows the solution to be sprayed within its confines, creating a salt fog environment around the coupons. Such a constantly moist, salty environment is quite aggressive.

G 85 describes modifications to B 117 involving a variety of solution chemistries and exposure regimens that can be used, including acetic acid-NaCl solution, acidified synthetic sea water, NaCl solution with $SO_2$ gas added and a 0.05 % NaCl + 0.35 % $(NH_4)_2SO_4$ solution. In addition, a variety of cycles (wet/dry) are described that have been found to be more aggressive than the constant moisture of B 117. In general, a spraying period is followed by a longer time at high relative humidity during which the sample can partially dry. However, standards such as G 85 lack a quantitative specification for relative humidity during dwell periods which can be strongly affected by the type of test chamber used. As relative humidity controls both equilibrium salt concentration as well as water layer thickness, localized corrosion rates as well as corrosion damage morphology will also be impacted by relative humidity levels. [12,13]

This cyclic type of exposure represents a more aggressive condition for most alloys than does constant, full immersion. Although still the subject of some debate, the generally accepted explanation involves the increased kinetics for oxygen reduction within the thin electrolyte layer that is present. Due to its limited solubility in water, oxygen reduction is usually under mixed or fully diffusion control for most alloys, particularly those undergoing stable pitting. The thin electrolyte layer present during wet/dry cycling increases the rate of delivery of oxygen to the surface by reducing the diffusion boundary layer thickness from ca. 0.08 cm [14] characteristic of stagnant solution to the thickness of the solution layer (often between 25 and 100 microns [15]). In addition, the concentration of aggressive ionic species increases dramatically during drying periods to the point of saturation.

Although realms of salt spray data exist, their use must be approached with care. As with ferric chloride, few industries actually operate in continuous salt spray (coastal regions and ships being notable exceptions). A number of industries have found that the standard salt spray testing not only does not reproduce the damage observed in service, but also is not particularly accelerating. Thus, the auto industry has developed a more complicated cyclic test, including an increase in the number of test intervals, known as GM 9540 [16] . The reasons for the discrepancies between service experience and these laboratory tests are not clear, and users of the test should bear them in mind.

*Coupon Exposures after Salt Loading*

As salt spray environments often do not to reproduce damage morphologies and rates seen in-service on alloys, coupon exposures under controlled relative humidity and temperature with a known loading density of salt have been used more recently. Multiple methods are used in order to deposit known salt loading densities on the surface of the alloys including a mixture of ethanol and saturated salt solutions [17–19] and inkjet printing [20–22]. When using ethanol, a whitish layer is seen on the surface of the alloy and the error in loading density is within 2 $\mu g/cm^2$ [19]. When a salt printer is used, the deposition of the salt is much more precise, seen in Fig. 1, with an error in loading of $\pm 0.1$ $\mu g/cm^2$ [21]. In both cases, the type of salt and corresponding loading density can be changed to match the environment of interest. After printing, the samples are put into controlled environments for the desired time of exposure. Akin to G85, cycles of relative humidity can be included in testing in order to mimic atmospheric conditions. In general, these exposure tests have a smaller water layer thickness than accelerated tests in ASTM standards and have the possibility to increase the diffusive flux of oxygen to the surface.

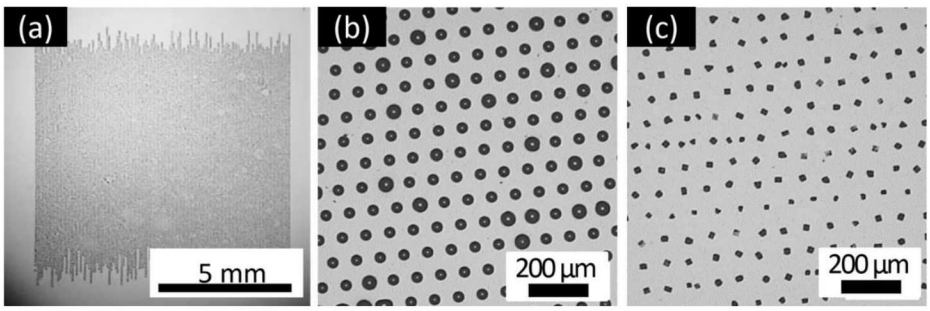


**Fig. 1- (a) printed droplet pattern on steel coupon, (b) detail of droplet pattern immediately after printing, (c) detail of**

**crystal pattern immediately after printing.**

*Droplet Exposures*

Along with controlled deposition of salt loading density, pitting can be studied under the small defined droplets of salt solutions. Micro-pipettes are used to place a small amount of liquid (on the order of μL's) onto the surface of an alloy and results in a droplet with a diameter in the range of a few mm's. After deposition, the samples can be placed under relative humidity and temperature control and left for a period of time[23,24]. Electrochemical measurements can be made inside the droplets using micro-electrodes to gain insights into the localized corrosion process in thin electrolyte layers [25]. The size and concentration of the salt in the drop is highly dependent upon the relative humidity in which the coupon is exposed in and can impact pitting that is seen on the surface [24]. However, the droplet can change size and volume through exposures or experimentation and further impact the results [25]. This needs to be considered when interpreting experimental results. A further consideration of droplet testing is the effect of the area for cathodic reduction reactions. When electrochemical reactions are occurring under the droplet, both the anode and the cathode must be contained in the droplet and thus can impact results from exposure testing.

*G 69 Standard Test Method for Measurement of Corrosion Potentials of Aluminum Alloys*

Aluminum alloys are highly susceptible to localized corrosion, including pitting. For many years, G 69 has been used to determine the so-called "solution potential" of Al alloys. The test solution described in G 69 is a strongly oxidizing, near-neutral pH chloride solution. The oxidizing power originates in the 3 g/L (0.09 M) hydrogen peroxide that is added. In the 1 M NaCl, virtually all precipitation-hardened Al alloys will undergo stable pitting. The solution potential measurement is made over a period of 1 h. It represents a mixed potential between the passive portions of the surface on which peroxide reduction is occurring and the pitting sites. Thus, the potential depends on (a) the cathodic kinetics of peroxide reduction, (b) the pit dissolution kinetics, and (c) the number and size of the pits. As these characteristics vary from alloy to alloy as well as with time, quantitative interpretation of the solution potential is challenging. Mixed potential theory can be used to demonstrate that the solution potential cannot be used to rank the resistance of Al alloys to stable pitting. Nonetheless, it has been used as a type of quality control test to probe batch-to-batch variations within a given alloy. This solution is also specified in G 110, a standard practice for evaluating intergranular corrosion of heat treatable aluminum alloys.

## Alteration of Test Methods

When considering how to accelerate a test, the two most commonly applied methods are to increase the temperature and/or increase the concentration of aggressive species (e.g., $Cl^-$ or H+). Either can be effective, and some of the electrochemical tests described below use the strong temperature dependence of pit stabilization as a parameter to quantify pitting resistance. That said, such changes must be introduced with care to ensure that the mechanism of attack in the accelerated test is the same as that in the actual service environment. Decreased time required for the testing should be balanced against the decreasing relevance of the results, and the consequential increase in the uncertainty in their interpretation. In addition, results from accelerated tests are useful for material selection, but not life prediction, as there is no means currently to connect the rates of pitting corrosion observed in these tests to other environments. This situation can be contrasted with crack growth testing where the similitude of the stress intensity factor, K, has been repeatedly demonstrated. This similitude allows results from laboratory scale test samples to be applied to service structures if the stress and flaw size and shape are known.

# ELECTROCHEMICAL TESTS

The main advantage of electrochemical testing is the opportunity to investigate corrosion phenomena in the solution of interest rather than in a (possibly) more aggressive and (probably) less relevant environment. In addition, a great deal of information can be gained about the dependence of the phenomena on external variables in a short time. Finally, the determination of critical potentials for initiation and propagation of localized corrosion can be useful in design decisions. For example, the use of mixed potential theory can allow prediction of the protection (either anodic or cathodic) criteria, as well as information on the galvanic couples to avoid.

### Specimen Mounting

One of the main challenges associated with electrochemical testing for localized corrosion resistance is sample mounting. It can be extremely difficult to mount a sample with an insulated electrical contact and a controlled exposed surface area without introducing a crevice at the sample/mount interface. Because crevice corrosion will occur at lower potentials than pitting, the sample invariably begins to be attacked at the crevice, leading to an underestimation of the resistance of the sample to pitting. Some may argue that for the same reason, this type of testing is not overly conservative, as in service, one wants to know the potential at which any localized corrosion can occur, not just pitting. The flaw in this argument is that most crevices formed during sample preparation are not reproducible either in position or geometry, making comparisons extremely difficult. In addition, there may be applications where crevice corrosion is not the failure mode of concern, but pitting is. Such testing with crevices present would lead one to choose a more resistant (and therefore more expensive) alloy than one would actually need.

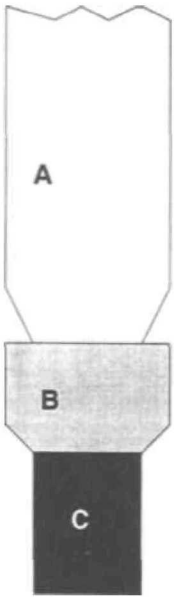


**Fig. 2 - Stern-Makrides electrode assembly. (A) glass tub that protects threaded steel rod from solution, (B) PTFE gasket, (C) specimen. For more details, see ASTM G5.**

A number of suggested solutions have been made for sample mounting, including the use of "knife-edge" Teflon washers [26], various mounting compounds and procedures [27], the use of wire loops [28], and flag geometries [29]. One experimental design even includes a crevice area that is continually washed with deionized water [30]. All of these have their limitations, and one must choose the most appropriate for the particular alloy/environment combination. The knife-edge PTFE washer, in combination with what has been known as the Stern-Makrides assembly (Fig. 2), has been used successfully in a number of applications in which a tight seal can be formed, which (a) prevents ingress of any electrolyte, and/or (b) causes the IR drop into the crevice to be so high as to prevent any polarization of the creviced surface away from $E_{corr}$. Because the latter of these is unlikely to occur, the prevention of ingress is critical. This prevention of solution ingress is closely related to the quality of the surface finish both in terms of its fineness (i.e., final polishing step particle size) and its uniformity. One large scratch can allow capillary action to draw electrolyte into an otherwise impervious crevice and start the crevice corrosion initiation process. This is the prime reason for the failings of this type of approach. In addition, due to the cost of the PTFE washers, many experimenters tend to try to reuse them. However, after the knife edge is deformed once, it will not form a watertight seal again, thus allowing crevice corrosion to occur.

The cell designed by Ovarfort [30,31] uses a slow flow (4 mL/min) of deionized water into the creviced area to prevent the accumulation of dissolution products inside the occluded area, the hydrolysis of which leads to crevice corrosion. The design has been successfully applied to the study of the pitting of a wide variety of stainless steels at both ambient and elevated temperature [30,31]. However, this cell can only be used for flat samples. In addition, one must be careful to ensure that the deionized water flow is uniform throughout the crevice. If a dead spot were to develop, crevice corrosion will very likely be initiated. Details of the cell can be found in Annex X2 of G150.

One example of the effect of crevices is shown in Fig. 3 for a 18Cr-8Ni stainless steel in a solution in which propagating crevice corrosion will not occur (1 N $H_2SO_4$) [27]. In this case, the higher passive current densities are observed for the insulating materials that perform poorly. In a $Cl^-$ containing solution, this would translate into a lower $E_{bd}$. As can be seen from Fig. 3, some mounting materials perform well in this solution, though it should be pointed out that these results cannot be extrapolated to other solutions. For example, the alkyd-varnish is used in electroplating to mask off areas that should not be plated. Although it works well in acid solutions, it performs very poorly in neutral or basic solutions, especially on materials with passive films such as stainless steel.

If mounting cannot be accomplished, three other approaches can be used. The first is the use of a wire loop electrode, as shown in Fig. 4a. Stockert et al. [28] have used this approach to study pitting without the complications of crevice corrosion. This approach works extremely well if one can get the material in wire form, though there is always the concern of metallurgical differences between material in wire form and that in plate or tube form, which are more likely to be used in engineering applications. A related approach is the use of a flag electrode configuration, as shown in Fig. 4b. This works well with plate material by minimizing the shaft size and thereby minimizing any effects of the waterline. If localized corrosion at the waterline continues to be a problem, deaeration of the solution and the air space above it can be of help as well. When deaerating, a baffle should be placed between the sample and the bubbler in order to prevent oscillations of the waterline. It should be noted that

flag electrodes can suffer edge attack that is not indicative of the behavior of the flat surface. Thus, post-test inspection of the location of the attack and careful interpretation of the results are important, as is the case for all electrochemical testing.

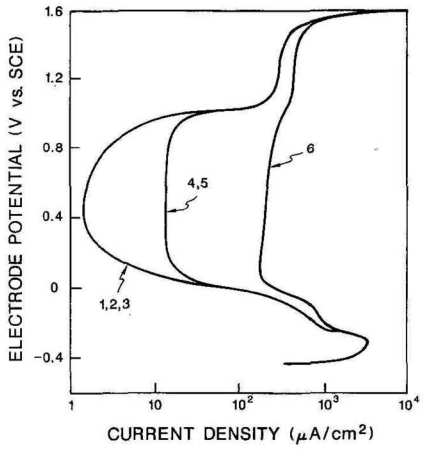


**Fig. 3 - Polarization curves of stainless steel in 1N sulfuric acid using different specimen mounting methods: (1) Stern-Makrides compression gasket, (2) heat-cured epoxy, (3) alkryd-varnish, (4) phenol-formaldehyde, (5) polymethyl methacrylate, (6) cold-cured epoxy.** [27]

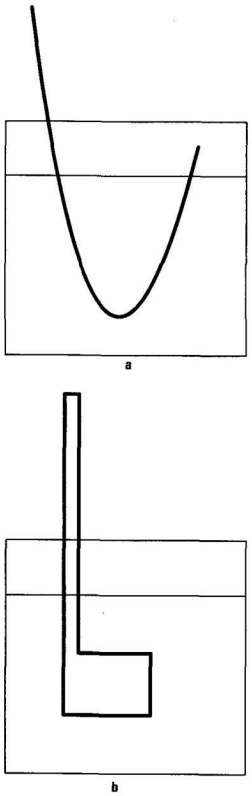


**Fig. 4 - (a) Wire loop configuration for electrochemical testing, (b) flag electrode configuration for electrochemical testing.**

Suter [32] developed a third approach to delineation of the surface area of interest. By using a microcapillary attached to a conventional optical microscope, Suter was able to define small areas of stainless steel surfaces and generate polarization curves. The area probed is defined by the diameter of the capillary with results demonstrated for capillaries between 2 and 1000 microns [33]. The cell is of particular use when the behavior a particular microstructural feature is of interest [34–36], as the design allows the matrix contribution to be minimized.

**Cyclic Polarization**

By far the most common electrochemical test for localized corrosion resistance is cyclic polarization. ASTM G 61, Test Method for Conducting Cyclic Potentiodynamic Polarization Measurements for Localized Corrosion Susceptibility of Iron-, Nickel-, or Cobalt-based Alloys, has been developed to allow experimenters to test their equipment and procedures on systems that are well characterized. The potential is scanned from $E_{corr}$ (or slightly below it) in the anodic direction until localized corrosion initiates as indicated by a large increase in the measured current density. At this point, the direction of the scan is reversed, and the current decreases until it changes polarity (i.e., becomes cathodic). Representative scans are shown in Fig. 5 for Type 304 SS and Hastelloy C-276. Conventional wisdom states that $E_{bd}$ (the breakdown potential) is the potential above which stable pits are initiated, while $E_{rp}$ (the repassivation potential) is the potential below which pits repassivate. The breakdown potential is usually defined as the potential at which there is a large increase in the applied current, whereas the repassivation potential is the potential on the reverse scan at which the applied anodic current becomes zero (i.e., the current changes polarity). Thus, the higher the value of $E_{bd}$, the more resistant is the alloy to the initiation of localized attack. The higher $E_{rp}$, the more easily the alloy can repassivate. At potentials between $E_{bd}$ and $E_{rp}$, sites that have initiated can propagate. Based upon this argument, one would favor an alloy that had both a high $E_{bd}$ and a high $E_{rp}$.

Examples of the range of data that can be expected are shown in the standard. The scatter in the data is apparent, especially in the forward scan. This scatter points out the statistical nature of the nucleation of pitting. The average $E_{bd}$ of Type 304SS was found to be approximately +0.15 V(SCE), while the average $E_{rp}$ was found to be approximately -0.21 V(SCE). The reverse scans are much more reproducible, because the local chemistry controls the repassivation. Another example of the inherent scatter in $E_{bd}$ is shown in Fig. 6 [37] for three variants of Type 304SS in 1000 ppm NaCl. The large variation in $E_{bd}$ arises despite the fact that all of the samples of each type were from the same heat of material and were tested under identical conditions.

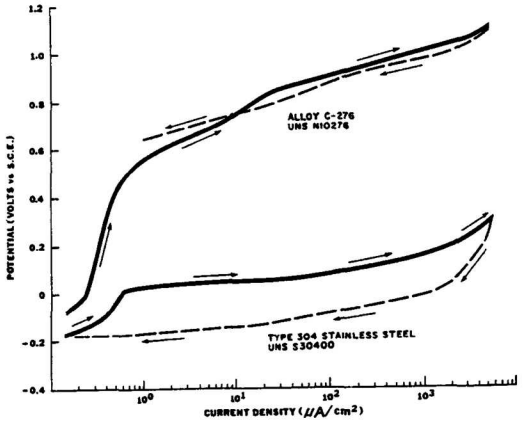


**Fig. 5 - Representative cyclic potentiodynamic polarization curves (ASTM G61). The average $E_{bd}$ for Type 304SS was approximately +0.15 $V_{SCE}$ while the average $E_{rp}$ was approximately -0.21 $V_{SCE}$.**

There have been numerous attempts to use the amount of hysteresis in the cyclic scan as a measure of localized corrosion susceptibility, with varying degrees of success. In this approach, the larger the hysteresis, the more likely a localized corrosion site will propagate once initiated. In the presence of a well-defined crevice, a good correlation has been found and the relative crevice corrosion susceptibility of alloys can be obtained. Wilde [38] demonstrated this for Hastelloy C, Incoloy 825 and Carpenter 20Cb3 in seawater where the amount of hysteresis correlated well with the amount of weight loss (due to crevice corrosion) in a two-year exposure to seawater. There is not a linear correlation, however, so local penetration rates cannot be predicted, but the test has been used successfully for alloy selection. However, in studies that have attempted to explore the relative pitting susceptibility of alloys, it has been found that comparisons are valid only if no crevices are present on any of the specimens tested. An example of the differences that one can observe is shown in Fig. 7. In the absence of crevices, the Fe-30Cr-3Mo alloy performs well in 1 M NaCl, with a high $E_{bd}$ and a small hysteresis. Microscopic examination showed the attack occurred only at the grain boundaries. However, when a crevice was intentionally applied, the alloy performed poorly. The possible problems in comparing one specimen that had a crevice with another that did not are obvious; incorrect conclusions concerning the relative resistance of two materials could easily be reached. Independent of the mounting method used, one should always examine the specimen for localized attack after the test is completed. At a minimum, microscopic examination of likely creviced areas should be performed. Some samples should be broken out of their mounts for more thorough examination.

While the interpretation of breakdown and repassivation potentials remains controversial, progress towards a consensus is being made. The large scatter in the breakdown potential is thought to be due to the sensitivity of pit initiation to the initial conditions. Its dependence on scan rate is most likely the result of the time dependence of the localized corrosion site chemistry development. In addition, it is now generally accepted that corrosion-resistant designs should not use $E_{bd}$ as the important

parameter, but the appropriate value of $E_{rp}$, because this is the potential below which pits should repassivate. Under these circumstances, the determination of the proper value of $E_{rp}$ becomes the focus.

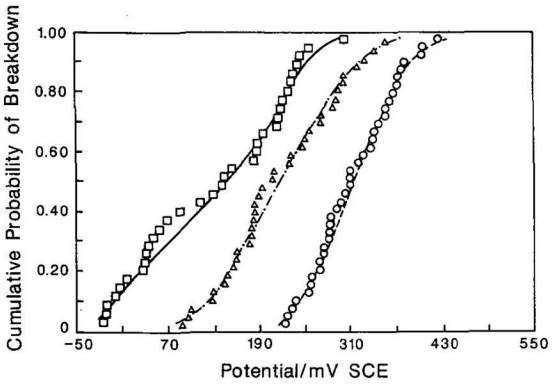


**Fig. 6 - Cumulative probability distributions of pitting breakdown potentials for three type 304 stainless steels in 1000 ppm NaCl with different sulfur contents: high sulfur (□) commercial purity (⩓), and high purity (○).**[37]

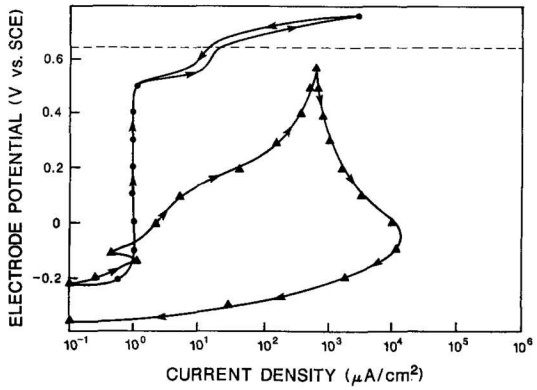


**Fig. 7 - Cyclic polarization curve for Fe-30Cr-3Mo alloy in dearated 1M NaCl for specimens (a) without a crevice (●), with a crevice (▲)** [38]**.**

Thompson and Syrett [39] attempted to address the problem of the proper pitting potential by performing a variety of electrochemical tests on Type 317L and Alloy 825 in simulated flue gas desulfurization environments to determine $E_{bd}$ and $E_{rp}$ as a function of the extent of pitting damage, characterized in terms of the time during which localized attack was allowed to occur. In terms of cyclic polarization, this time would be inversely proportional to the sweep rate on the reverse portion of the scan, with lower sweep rates leading to greater attack. As shown in Fig. 8 for Type 317L, their results indicate the convergence of $E_{bd}$ and $E_{rp}$ at a single potential of +0.2 V(SCE). This "unique potential" can be interpreted as the potential below which the smallest pit will neither initiate nor grow. Quantifying the size of the "smallest" pit remains an important task. However, the work is important support for the hope of eventually developing quantitative, engineering-relevant criteria for material selection against pitting.

One of the historical controversies with regard to $E_{rp}$ as a "material property" are the results of Wilde [38] in which the repassivation potential was shown to depend to some extent on the amount of localized dissolution that has been allowed to occur, and therefore depends on both the scan rate and the current at which the scan is reversed. The more attack that has been allowed to occur, the more negative is the $E_{rp}$. However, there are other data on stainless steels that show a limiting value for large pits (0.05-0.5 mm deep) [40,41], complementing the work of Thompson and Syrett [39], where a limiting value is also found for small pits.

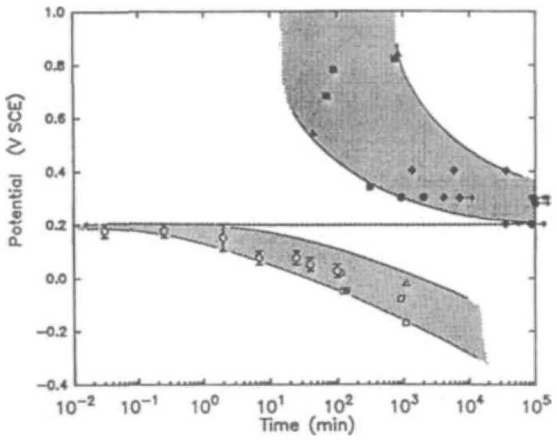


**Fig. 8 - Critical potentials ($E_{bd}$ and $E_{rp}$) for type 317L stainless steel exposed to a simulated flue gas desulfurization environment as a function of the time during which localized corrosion was allowed to propagate before repassivation occurred. Symbols denote different methods used to determine values: cyclic polarization (filled and open squares and triangles); constant potential tests (filled and open circles and diamonds)** [39]**.**

Despite the problems, polarization testing is useful for comparing alloys with respect to propagation of localized corrosion, though its use gives little information on the initiation time that is necessary for accurate lifetime prediction. One alloy may have superior resistance to propagation, but have much inferior resistance to initiation, and thus result in a shorter application lifetime.

**Galvanostatic Measurements**

Controlled current tests for pitting are seeing increased popularity. Galvanostatic measurements involve the application of a series of small, step changes in the applied current. The potential is followed as the current is increased as described in ASTM G 100, Method for Conducting Cyclic Galvanostaircase Polarization. In some cases, more reproducible values for $E_{rp}$ can be obtained galvanostatically in some systems, notably aluminum in inhibited water [42]. However, potential oscillations at constant current can sometimes occur, which, while of scientific interest, can make interpretation of the results difficult, as the choice of potential becomes almost arbitrary.

**Potentiostatic Measurements**

By far the most common electrochemical tests used is cyclic polarization. Nonetheless, potentiostatic measurements can be powerful tools in evaluating pitting behavior. Ideally, potentiostatic tests would be conducted over long time periods to avoid being fooled by long initiation times. Potentiostaircase tests can be performed in lieu of potentiodynamic tests, though, at equivalent potential scan rates, the results should be identical. Unfortunately, long-term potentiostatic testing is extremely time-consuming and expensive. In addition, the time frames involved are usually still very short compared to the projected life. Thus, a number of approaches have been developed for accelerating the process of initiation.

Mechanical scratching is favored by some as a means by which a bare surface can be created. In this technique, one is ascribing no importance to initiation time. The surface is held at a constant potential and then a portion of it is scratched, usually with a diamond-tipped stylus. The current is monitored with time. For potentials below $E_{rp}$, the surface will repassivate rather rapidly, as shown in Fig. 9. Just above $E_{rp}$, the surface will try to repassivate, but will fail, and the current will eventually increase. The closer the potential to $E_{rp}$, the longer is the time before the current increases. Thus, in most cases, the $E_{rp}$ measured by this method is not conservative, as usually no more than 10 min is spent at any one potential. If one had waited long enough at the potential used just before the measured $E_{rp}$, localized corrosion might have occurred. However, this does not denigrate its utility as a screening test. One problem with scratching tests of this type is the dependence on the weight of the scratch. For scratching by hand, the $E_{rp}$ decreases with increasing damage. A mechanical system improves the reproducibility. A more difficult problem concerns the site of pitting. In many cases, pitting occurs at inclusions or second-phase particles of one type or another. Such inclusions are usually present at small volume fractions, so the probability of scratching across one (or more) with a fine diamond tip is extremely small. This paucity of sites can lead to erroneously high values of $E_{rp}$ which reflect the pitting susceptibility of the matrix material, but ignore the susceptibility of the weakest link, the inclusions.

There are also purely electrochemical methods that can be used to produce a bared surface. In one technique, the entire exposed surface is activated by a large positive voltage excursion, which is followed by a voltage step back to (or towards) $E_{corr}$. In this way, any potential pitting sites are initiated, and the test measures the ability of the material to resist propagation and to repassivate. One version of this test (Fig. 10) involves a step to +2 V for 3 s followed by a step back to $E_{corr}$, during which time the current is monitored. The potential is held there for 5 min before it is again stepped to +2 V for 3 s to reinitiate localized corrosion. At this point, the potential is stepped back to a potential 50 mV above $E_{corr}$ and the current is monitored for 5 min. The process is repeated until the current does not decay upon the step in the negative direction. In this way, an estimate of $E_{rp}$

can be made, with better estimates resulting from the use of smaller increments in the test potential (e.g., 25 mV instead of 50 mV). This method is essentially using the potentiostat to "electrochemically scratch" the specimen surface. A related method is described in ASTM F 746, Test Method for Pitting or Crevice Corrosion of Metallic Surgical Implant Materials, for determining the pitting and crevice corrosion susceptibility of materials used in medical implants.

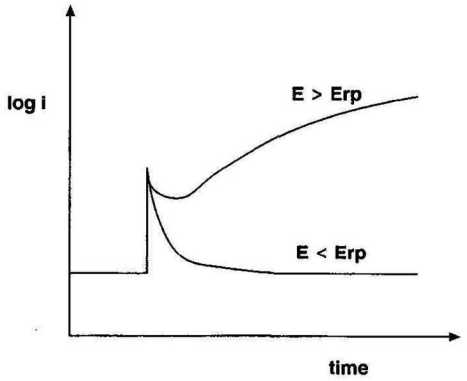


**Fig. 9 - Scratch test current-time curves for a specimen held potentiostatically above the repassivation potential ($E_{rp}$) and below $E_{bd}$.**



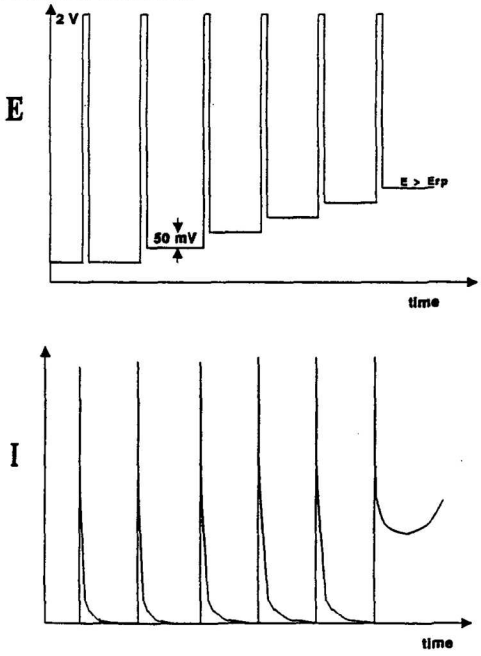


**Fig. 10 - Schematic E(t) and I(t) for electrochemical scratch method for determining the repassivation potential.**

In another electrochemical test that focuses on pit propagation, the potential is scanned at 10 mV/s to a potential E1 between $E_{bd}$ and $E_{rp}$ where it is held to determine the background passive current density. After 10 min, the potential is scanned anodically past $E_{bd}$ until the current density is 10 mA/cm$^2$, at which time the potential is stepped back to E1. The current is then monitored for 10 min, after which the potential is held at $E_{corr}$ for 5 min to repassivate the pits. Finally, the potential is stepped back to E1 and the current is monitored to ensure that the background current has not changed appreciably. The amount of charge passed during the propagation stage is compared to the pitted area (determined by optical microscopy) to determine an average pit penetration rate. This test is known as the Pit Propagation Rate (PPR) Test [43].

Frankel [44,45] has developed a means of testing pit propagation using thin foils. The geometry of the foil restricts the dissolution to two spatial dimensions, allowing optical measurements of changes in diameter to be related to the measured current, thereby establishing an accurate rate of pit propagation as well as conditions under which such pits repassivate. The method has been applied to sputtered Al thin films [45] as well as Al alloys[44]. The primary experimental challenge is the creation of foils that are sufficiently thin to produce a stable, two-dimensional pit. While sputter deposition is an excellent

method, the production of thin foils of engineering alloys provides more of a challenge, although not always an insurmountable one.

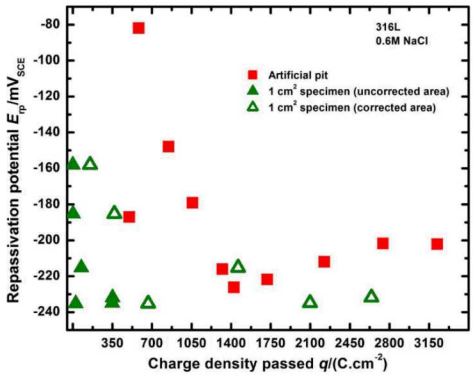


**Fig. 11 – Repassivation potential of 1-dimensional reference electrodes in comparison to CPP experiments** [46]**.**

Along with two-dimensional dissolution in foils, insights into pit propagation and repassivation can also be made through electrochemical measurements on artificial pits formed by embedding wire (usually on the order of 50 µm diameter) in an insulating material restricting the geometry to one spatial dimension [47,48]. By leaving a cross-section of the wire exposed to solution, a potentiostatic anodic hold will allow for the entire interfacial area to be active. Dissolution of the wire is in one-dimension, therefore, modeling the effects of mass transfer are straight forward as given by the original formulism of Galvele [48,49]. These one-dimensional electrodes can be used to measure conditions for pit propagation, namely the pit stability product, $(i \cdot x)$, where $i$ is the current density and $x$ is the pit depth. A critical value of $i \cdot x$ describes the current density needed to continue propagation at any given depth, $x$. $E_{rp}$ can also be measured with one-dimensional electrodes, as limiting values for $E_{rp}$ have are reached at sufficient depth (charge passed) as seen in Fig. 11 [40,50] further complementing the work of Thompson and Syrett [39]. These $E_{rp}$ values are not affected by the dissolution products created during the 1D pit growth due to the small amount of charge needed, as compared to macro-sized electrodes. Artificial pit electrodes can be used to gain insights into pit propagation and repassivation in different alloys [50,51] as well as to quantify solution and temperature effects [52–54]. Measurements for pit stability are generally made under the presence of a salt film, however, pitting has been shown to occur when a salt film is not present on the surface of a pit and thus a critical value of the fraction of saturation at the pit surface required for propagation is also needed, limiting the direct application of this parameter [47].

**Critical Temperature Tests**

Although ASTM tests use temperature to accelerate attack during exposures, temperature can also be used in combination with electrochemical techniques. One example of this is the determination of critical pitting temperatures (CPT) [31,55,56] for alloy development or selection, or both. An anodic potential is applied to an electrode at low temperature (room or below) in the solution of interest and the temperature slowly increases in order to determine the temperature at which initiation of localized corrosion occurs, as signified by an increase in the current above some criterion. Such a method allows a quantitative ranking of materials in terms of resistance to pitting. It is important to recognize that CPT does not represent an intrinsic material property but rather a statistically distributed value that is dependent on material surface condition, test exposure area and test environment [54].

ASTM G 150 (Standard Test Method for Electrochemical Critical Pitting Temperature Testing of Stainless Steels) describes in detail how to perform such experiments. The solution prescribed is 1 M NaCl, the suggested applied potential is +700 mV(SCE) and the starting temperature is deemed to be 0°C, with the temperature being increased at l˚C/min. The CPT is defined as the temperature at which the current exceeds 100 µA/cm$^2$ and remains so for greater than 1 min. The test method clearly states that alternative potentials can be used if they are within the range for which the CPT is potential independent.

Salinas-Bravo and Newman [57] developed variation on the critical pitting temperature test for welded stainless steels in which a large, unwelded specimen was coupled to a welded sample via a zero resistance ammeter (ZRA). The unwelded specimen polarizes the welded sample to a positive potential. As the temperature is raised, the galvanic current between the two remains low until the CPT is reached. At that point, the welded sample undergoes stable pitting and a large current is observed. The attractiveness of this test is that it probes the inherent galvanic couple that is the essence of localized corrosion: the large, passive cathode, and the small, active pit.

**Electrochemical Noise**

Electrochemical noise has seen increased interest as a tool for both corrosion science and corrosion engineering. By monitoring the galvanic current between two nominally identical electrodes or the corrosion potential of a single electrode carefully, metastable pitting can be detected. The localization of the dissolution inherent in localized corrosion implies a separation of the anodic and cathodic reactions that constitute the corrosion couple. This physical separation of reactions distinguishes localized corrosion from uniform corrosion in which it is traditionally thought that the anodic and cathodic sites are in very close

proximity to one another. The majority of the anodic (oxidative dissolution) reaction occurs inside the localized corrosion site, while the majority of the cathodic (reduction) reaction occurs on the boldly exposed surface. Thus, a galvanic couple is created. The spatial separation of the processes necessitates the passage of current between the two sites. This passage of current leads to the various electrochemical noise signals measured.

Under open circuit conditions, bursts of dissolution at localized corrosion sites require the generation of bursts of cathodic current from the surrounding boldly exposed surface. This increased demand typically causes a decrease in the measured open circuit potential. Localized corrosion sites are typically very small (<100 μm diameter). However, the current densities inside these cavities during transient bursts can be on the order of 1 A/cm$^2$. These rates are possible because of the extremely aggressive environments that develop inside localized corrosion sites. Thus, even though the sites are geometrically small, they can influence the electrochemical potential of the much larger boldly exposed surface on which the electrode kinetics are far slower. This difference in relative current densities on separated anodes and cathodes is what accounts for the ability to detect the electrochemical noise associated with localized corrosion. When the potential of the surface is controlled with an external device, the same burst of dissolution requires the device to supply a burst of current, which can be recorded. Usually, these bursts are transient, with temporary repassivation of the localized corrosion site occurring and allowing the system to return to the previous steady-state condition. On a metal surface of appreciable size (>1 cm$^2$), there can be many localized corrosion sites. They will usually propagate independently, so that a series of current (or potential) fluctuations is observed due to the summation of the signals from the individual sites. These fluctuations are referred to as "electrochemical noise." Because electrochemical noise can be observed often under open circuit conditions, it has been hailed as the only truly noninvasive electrochemical method. Several methods for *in-operando* corrosion monitoring based on these concepts are overviewed in ASTM G199 (Standard Guide for Electrochemical Noise Measurement). Changes in the noise signal are often taken as an indication that conditions are favorable for pit initiation to occur. Thus, if one is monitoring a process stream, corrective action can be taken. Numerous data analysis procedures for electrochemical noise signals have been proposed for the identification of pitting conditions, some of which are described in ASTM G199. The theoretical basis for these analysis approaches is often not well defined and the reliability can be highly variable depending on approach and the conditions of the system being monitored[58,59]. Relatedly, another disadvantage of noise monitoring is that it does not give sufficient information about what level of this metastable pitting is acceptable. For example, there may be literally millions of metastable pits forming and repassivating in a vessel wall, but only one needs to penetrate completely for a leak to develop. It may not be possible to differentiate between conditions that will allow that and those in which the extent of pitting is negligible. Experience and correlations with coupon exposures are critical factors in the use of noise for localized corrosion monitoring. A guide has been provided by Huet and Ngo for improving measurements and data analysis for electrochemical noise measurements [60].

**Acoustic Emission Monitoring of Corrosion**

Acoustic Emission (AE) testing is a non-destructive technique aimed toward understanding localized corrosion as it occurs. The basics of AE involve the detection of micro-signals from growing corrosion damage by converting very small surface displacement to a voltage and can be collected as a function of time. The AE signals have been correlated to the number of pits that are present on the surface of the alloy [61] along with other uses detailed in work by Wu et al. [62]. This technique can be very sensitive and allows for detection of very small perturbations, however, is also a downfall of the technique as deconvolution from ambient vibrations can be rather difficult. There are many sources of vibrations on the surface of a material during corrosion including: (i) bubbling from H2 evolution, (ii) initiation events due to passive film rupture and (iii) pit propagation. Along with these problems, it is likely that an area under study could have multiple pitting events at different stages of the pitting process and therefore convolute the AE signal.

**Scanning Techniques Applied to Localized Corrosion**

Although a detailed overview of various scanning techniques is beyond the scope of this chapter, a quick summary of advantages and disadvantages to each technique along with the capabilities will be outlined. There are various scanning techniques that are commonly used including: scanning Kelvin probe (SKP), scanning Kelvin probe force microscopy (SKPFM), Scanning vibrating electrochemical technique (SVET), and scanning electrochemical microscopy (SECM). SKP is characterized by measuring two-dimensional distributions of the contact potential difference between the tip and the surface of interest. The SKP can be combined with atomic force microscopy to create an SKPFM and results in simultaneous mapping of the surface topography as well as the potential difference [63]. The resolution of these techniques varies and SKPFM can be on the order of the nm while SKP is generally limited by the tip size and distance between the tip and the sample. Due to the small resolution, SKP and SKPFM are useful in determining the propensity for pit initiation sites. SVET measures local current potential in solution to map electrochemical currents above the surface of corroding metals and allows for the determination of local cathodic and anodic regions of interest. SVET has a much lower spatial resolution than SKP and SKPFM at about 100-200 μm and has a current density resolution around 1 μA/cm$^2$ [64]. The user should also be aware that when using these methods for *in-situ* measurements, the solution is stirred causing mixing of the localized solution and can change diffusion. SECM electrolysis current that flows at a microelectrode immersed in solution is moved above an alloys surface and is used to characterized electrochemical processes [65]. When considering all scanning techniques, localized corrosion is characterized by

a stochastic process which can occur on very short time scales. When scanning a surface in the presence of an electrolyte, it is possible that these events are either missed or are in the stages of initiation/repassivation and could impact the results.

## PREDICTIVE CAPABILITIES

With the caveats mentioned previously in mind, the study of metastable pitting can be used to assist in lifetime prediction studies. If pitting is truly a stochastic phenomenon, then one can apply statistics to allow prediction of the likelihood of pit propagation, given sufficient information. The information needed is (a) the probability that a pit will nucleate under a given set of conditions, and (b) the probability that once a pit nucleates, it will survive (*i.e.*, become stable). Such information could be used to estimate component lifetimes, which could then be used to make design decisions based on the consequences of a failure. For example, a 3% chance of perforation may be acceptable for an easily shutdown and repaired vessel if it allows a cheaper alloy to be used, but such a probability would not be acceptable for a critical component in an inaccessible submersible.

Analyses of these current and potential transients due to metastable pits can provide information regarding the controlling factors and their dependence on environmental, metallurgical, and applied potential conditions. For example, Pride et al. [66] characterized the metastable pitting behavior of high-purity Al and aged Al-2%Cu. They found that the frequency of pitting events was proportional to both the applied potential and the chloride concentration. The rate of pitting was also found to decrease with increasing exposure time. These kinds of analyses can serve as the basis for the pitting prediction methodologies described below.

Shibata et al. [8] and Williams et al. [67] have applied such statistical arguments to pitting of stainless steel. To develop these models, a large amount of data that can be treated as an ensemble must be gathered. In other words, variations in results from test to test are expected, even for nominally identical tests. This variation is used to develop the cumulative probability curve for pitting under a certain set of conditions. Both groups used multiple specimen testing apparatus to gather up to 12 data points for critical potentials and metastable pit nucleation rates simultaneously. The results for one set of 30 tests are shown in Fig. 6 [37]. This shows that the breakdown potential $E_{bd}$ follows a distribution. Thus, there is a 20% chance that the breakdown potential of commercial 304 SS will be below +160 mV(SCE) in 1000 ppm NaCl. The argument is that there was nothing "wrong" with those tests whose $E_{bd}$ was less than +160 mV(SCE), but that the variation reflects the stochastic nature of the pitting process. Qualitatively similar data have been developed for Al alloys and their constituent second phase particles [68].

The development of commercially available multipotentiostats has made measurements of pitting conditions and the underlying factors more tractable. Lunt et al. [69] used an array of nominally identical electrodes to characterize the strengths and extent of the types of interactions that occur among active pits. In addition, such instrumentation makes the determination of the statistical distribution of pitting potentials via the testing of a large number of specimens much less time intensive, as multiple electrodes (up to 100) [70] can be independently tested simultaneously.

## CONCLUDING REMARKS

The goals of this chapter were to give a brief overview of the exposure tests used to determine localized corrosion susceptibility, and to introduce a variety of electrochemical techniques that can provide important information concerning localized corrosion susceptibility. Although none of the methods is perfect or a panacea, when used judiciously and in combination, a better picture of the localized corrosion process can be gained, even in complicated solutions. This allows for more informed decisions on alloy selection, process alteration, or failure analysis. While prediction of localized penetration rate remains a goal of electrochemical testing, applications of statistics to the process appear promising.

**Acknowledgements**

Sandia National Laboratories is a multi-mission laboratory managed and operated by National Technology and Engineering Solutions of Sandia, LLC., a wholly owned subsidiary of Honeywell International, Inc., for the U.S. Department of Energy's National Nuclear Security Administration under contract DE-NA0003525

**REFERENCES**

[1] Szlarska-Smialowska, Z., "Pitting Corrosion of Metals", *NACE*, 1986
[2] Frankel, G. S., "Pitting Corrosion of Metals. A Review of the Critical Factors", *Journal of The Electrochemical Society*, Vol. 145, 1998, p. 2186–2198
[3] Soltis, J., "Passivity breakdown, pit initiation and propagation of pits in metallic materials - Review", *Corrosion Science*, Vol. 90, 2015, p. 5–22
[4] *Corrosion Tests and Standards: Application and Interpretation, Manual 20 (Sec. III, Types of Tests)*, West Conshohocken, PA, 1995
[5] Ailor, W. H., Ed., *Handbook On Corrosion Testing and Evaluation*, John Wiley & Sons Inc., New York, 1971
[6] Streicher, M. A., "Pitting Corrosion of 18Cr-8Ni Stainless Steel", *Journal of The Electrochemical Society*, Vol. 103, 2007, p. 375
[7] Ernst, P., Laycock, N. J., Moayed, M. H., and Newman, R. C., "The mechanism of lacy cover formation in pitting", *Corrosion Science*, Vol. 39, 1997, p. 1133–1136

[8] Shibata, T. and Takeyama, T., "Stochastic Theory of Pitting Corrosion", *Corrosion*, Vol. 33, 1977, p. 243–251
[9] Aziz, P. M. and Godard, H. P., "Influence of Specimen Area on the Pitting Probability of Aluminum", *Journal of The Electrochemical Society*, Vol. 102, 1955, p. 577–579
[10] ASTM International, "G004 - Standard Guide for Conducting Corrosion Tests in Field Applications", *ASTM International*, 2014, p. 1–10
[11] ASTM International, "ASTM G50 - Standard Practice for Conducting Atmospheric Corrosion Tests on Metals 1", 2015, p. 1–11
[12] Parker, M. B. and Kelly, R. G., "Improved Atmospheric Corrosion Testing for Aluminum Alloys Part I: Deconstructing ASTM G85-A2", *Corrosion*
[13] Parker, M. B. and Kelly, R. G., "Improved Atmospheric Corrosion Testing for Aluminum Alloys Part II: Developing Improved Testing Protocol", *Corrosion*
[14] Liu, C., Srinivasan, J., and Kelly, R. G., "Electrolyte Film Thickness Effects on the Cathodic Current Availability in a Galvanic Couple", *Journal of The Electrochemical Society*, Vol. 164, 2017, p. C845–C855
[15] Leygraf, C. and Graedel, T. E., in, p. 11, Wiley and Sons
[16] Singleton, R., *Corrosion: Fundamentals, Testing and Protection, ASM Handbook*, p. 470, ASM International, Materials Park, OH
[17] Lindström, R., Svensson, J.-E., and Johansson, L. G., "The Influence of Salt Deposits on the Atmospheric Corrosion of Zinc. The Important Role of the Sodium Ion", *Journal of The Electrochemical Society*, Vol. 149, 2002, p. B57–B64
[18] Li, S. and Hihara, L. H., "Aerosol salt particle deposition on metals exposed to marine environments: A study related to marine atmospheric corrosion", *Journal of the Electrochemical Society*, Vol. 161, 2014, p. 268–275
[19] Strandberg, H. and Johansson, L.-G., "Electrochemical aspects of copper atmospheric corrosion in the presence of sodium chloride", *Journal of The Electrochemical Society*, Vol. 145, 1998, p. 1093–1100
[20] Schindelholz, E. J. and Kelly, R. G., "Application of Inkject Printing for Depositng Salt Prior to Atmospheric Corrosion Testing", *Electrochemical and Solid-State Letters*, Vol. 13, 2010, p. C29–C31
[21] Schindelholz, E., Risteen, B. E., and Kelly, R. G., "Effect of Relative Humidity on Corrosion of Steel under Sea Salt Aerosol Proxies", *Journal of The Electrochemical Society*, Vol. 161, 2014, p. C450–C459
[22] Schindelholz, E., Tsui, L. K., and Kelly, R. G., "Hygroscopic particle behavior studied by interdigitated array microelectrode impedance sensors", *Journal of Physical Chemistry A*, Vol. 118, 2014, p. 167–177
[23] Guo, L. et al., "Effect of mixed salts on atmospheric corrosion of 304 stainless steel", *Journal of the Electrochemical Society*, Vol. 166, 2019, p. C3010–C3014
[24] Tsutsumi, Y., Nishikata, A., and Tsuru, T., "Pitting corrosion mechanism of Type 304 stainless steel under a droplet of chloride solutions", *Corrosion Science*, Vol. 49, 2007, p. 1394–1407
[25] Hangarter, C. M. and Policastro, S. A., "Electrochemical Characterization of Galvanic Couples Under Saline Droplets in a Simulated Atmospheric Environment", *Corrosion*, Vol. 9312, 2017, p. 268–280
[26] Stern, M. and Makrides, A. C., "Electrode Assembly for Electrochemical Measurements", *Journal of The Electrochemical Society*, Vol. 107, 1960, p. 782
[27] Greene, N. D., France, W. D., and Wilde, B. E., "Electrode Mounting for Potentiostatic Anode Polarization Studies", *Corrosion*, Vol. 21, 1965, p. 275
[28] Stockert, L., Hunkeler, F., and Bohni, H., "Crevice-Free Measurement Technique To Determine Reproducible Pitting Potentials", *Corrosion*, Vol. 41, 1985, p. 676–677
[29] Shaw, B., thesis, Johns Hopkins University
[30] Ovarfort, R., "New electrochemical cell for pitting corrosion testing", *Corrosion Science*, Vol. 28, 1988, p. 135–140
[31] Ovarfort, R., "Critical pitting temperature measurements of stainless steels with an improved electrochemical method", *Corrosion Science*, Vol. 29, 1989, p. 987–993
[32] Suter, T. and Bohni, H., "Microelectrodes for corrosion studies in microsystems", *Electrochimica Acta*, Vol. 47, 2001, p. 191–199
[33] Park, J. O., Suter, T., and Böhni, H., "Role of manganese sulfide inclusions on pit initiation of super austenitic stainless steels", *Corrosion*, Vol. 59, 2003, p. 59–67
[34] Staemmler, L., Suter, T., and Böhni, H., "Glass Capillaries as a Tool in Nanoelectrochemical Deposition", *Electrochemical and Solid-State Letters*, Vol. 5, 2002, p. C61–C63
[35] Suter, T. and Alkire, R. C., "Microelectrochemical Studies of Pit Initiation at Single Inclusions in Al 2024-T3", *Journal of The Electrochemical Society*, Vol. 148, 2001, p. B36–B42
[36] Leard, R. R. and Buchheit, R. G., "Electrochemical Characterization of Copper-Bearing Intermetallic Compounds and Localized Corrosion of Al-Cu-Mg-Mn Alloy 2024", *Materials Science Forum*, Vol. 396–402, 2002, p. 1491–1496
[37] Stewart, J., thesis, University of Southampton, U.K.
[38] Wilde, B. E., *Localized Corrosion* R. W. Staehle, B. F. Brown, J. Kruger, and A. Agarwal, Editors, p. 342, NACE, Houston, TX, 1974
[39] Thompson, N. G. and Syrett, B. C., "Relationship between conventional pitting and protection potentials and a new, unique pitting potential", *Corrosion*, Vol. 48, 1992, p. 649–659

[40] Sridhar, N. and Cragnolino, G. A., "Applicability of Repassivation Potential for Long-Term Prediction of Localized Corrosion of Alloy-825 and Type-316L Stainless-Steel", *Corrosion*, Vol. 49, 1993, p. 885–894
[41] Hakkareinen, T., *Passivity of Metals and Semiconductors* M. Forment, Editor, p. 367, Elsevier Science Publishers B.V., Amsterdam, The Netherlands, 1983
[42] Hirozawa, S. T., *Laboratory Corrosion Tests and Standards, ASTM STP 866* G. S. Haynes and R. Babojan, Editors, p. 108, ASTM International, West Conshohocken, PA, 1958
[43] Syrett, B. C., "PPR Curves - A new method of assessing pitting corrosion resistance", *Corrosion*, Vol. 33, 1977, p. 221
[44] Sehgal, A., Frankel, G. S., Zoofan, B., and Rokhlin, S., "Pit Growth Study in Al Alloys by the Foil Penetration Technique", *Journal of The Electrochemical Society*, Vol. 147, 2000, p. 140–148
[45] Frankel, G. S., Newman, R. C., Jahnes, C. V, and Russak, M. A., "On the Pitting Resistance of Sputter-Deposited Aluminum Alloys", *Journal of The Electrochemical Society*, Vol. 140, 1993, p. 2192–2197
[46] Srinivasan, J., McGrath, M. J., and Kelly, R. G., "A High-Throughput Artificial Pit Technique to Measure Kinetic Parameters for Pitting Stability", *Journal of The Electrochemical Society*, Vol. 162, 2015, p. C725–C731
[47] Laycock, N. J. and Newman, R. C., "Localised dissolution kinetics, salt films and pitting potentials", *Corrosion Science*, Vol. 39, 1997, p. 1771–1790
[48] Newman, R. C., Ajjawi, M. A. A., Ezuber, H., and Turgoose, S., "An experimental confirmation of the pitting potential model of galvele", *Corrosion*, Vol. 28, 1988, p. 471–477
[49] Galvele, J. R., "Transport Processes and the Mechanism of Pitting of Metals", *Journal of The Electrochemical Society*, Vol. 123, 1976, p. 464–474
[50] Srinivasan, J. and Kelly, R. G., "On a recent quantitative framework examining the critical factors for localized corrosion and its impact on the galvele pit stability criterion", *Corrosion*, Vol. 73, 2017, p. 613–633
[51] Li, T., Scully, J. R., and Frankel, G. S., "Localized Corrosion: Passive Film Breakdown vs. Pit Growth Stability: Part III. A Unifying Set of Principal Parameters and Criteria for Pit Stabilization and Salt Film Formation", *Journal of The Electrochemical Society*, Vol. 165, 2018, p. C762–C770
[52] Jun, J., Frankel, G. S., and Sridhar, N., "Further Modeling of Chloride Concentration and Temperature Effects on 1D Pit Growth", *Journal of The Electrochemical Society*, Vol. 163, 2016, p. C823–C829
[53] Moayed, M. H. and Newman, R. C., "The Relationship Between Pit Chemistry and Pit Geometry Near the Critical Pitting Temperature", *Journal of The Electrochemical Society*, Vol. 153, 2006, p. 330–335
[54] Li, T., Scully, J. R., and Frankel, G. S., "Localized Corrosion: Passive Film Breakdown vs Pit Growth Stability: Part II. A Model for Critical Pitting Temperature", *Journal of The Electrochemical Society*, Vol. 165, 2018, p. C484–C491
[55] Brigham, R. J., "Temperature as a Pitting Criterion", *Corrosion*, Vol. 29, 1973, p. 33–36
[56] Lau, P. and Bernhardsson, S., *Electrochemical Techniques in Corrosion Engineering* R. Baboian, Editor, p. 281, NACE, Houston, TX, 1986
[57] Salinas-Bravo, V. M. and Newman, R. C., "An alternative method to determine critical pitting temperature of stainless steels in ferric chloride solution", *Corrosion Science*, 1994
[58] Homborg, A. M. et al., "A critical appraisal of the interpretation of electrochemical noise for corrosion studies", *Corrosion*, Vol. 70, 2014, p. 971–987
[59] Al-Mazeedi, H. A. A. and Cottis, R. A., in *Electrochimica Acta*,
[60] Huet, F. and Ngo, K., "Electrochemical Noise - Guidance for improving measurements and data analysis", *Corrosion*, Vol. 75, 2018, p. 1065–1073
[61] Mazille, H., Rothea, R., and Tronel, C., "An acoustic emission technique for monitoring pitting corrosion of austenitic stainless steels", *Corrosion Science*, Vol. 37, 1995, p. 1365–1375
[62] Wu, K., Jung, W. S., and Byeon, J. W., "In-situ monitoring of pitting corrosion on vertically positioned 304 stainless steel by analyzing acoustic-emission energy parameter", *Corrosion Science*, Vol. 105, 2016, p. 8–16
[63] Efaw, C. M. et al., "Toward improving ambient Volta potential measurements with SKPFM for corrosion studies", *Journal of the Electrochemical Society*, Vol. 166, 2019, p. C3018–C3027
[64] Bastos, A. C., Quevedo, M. C., Karavai, O. V., and Ferreira, M. G. S., "Review - On the application of the scanning vibrating electrode technique (SVET) to corrosion research", *Journal of the Electrochemical Society*, Vol. 164, 2017, p. C973–C990
[65] Bard, A. J., Fan, F. R. F., Kwak, J., and Lev, O., "Scanning Electrochemical Microscopy. Introduction and Principles", *Analytical Chemistry*, Vol. 61, 1989, p. 132–138
[66] Pride, S. T., Scully, J. R., and Hudson, J. L., "Metastable Pitting of Aluminum and Criteria for the Transition to Stable Pit Growth", *Journal of The Electrochemical Society*, Vol. 141, 1994, p. 3028–3040
[67] Williams, D. E., Westcott, C., and Fleischmann, M., "Stochastic Models of Pitting Corrosion of Stainless Steels - II. Measurement and Interpretation of Data at Constant Potential", *Journal of The Electrochemical Society*, Vol. 132, 1985, p. 1804–1811
[68] Ilevbare, G. O., Scully, J. R., Yuan, J., and Kelly, R. G., "Inhibition of pitting corrosion on aluminum alloy 2024-T3: Effect of soluble chromate additions vs chromate conversion coating", *Corrosion*, Vol. 56, 2000, p. 227–242
[69] Lunt, T. T., Scully, J. R., Brusamarello, V., Mikhailov, A. S., and Hudson, J. L., "Spatial Interactions among Localized Corrosion Sites Experiments and Modeling", *Journal of The Electrochemical Society*, Vol. 149, 2002, p.

B163–B173
[70] Budiansky, N. D., Hudson, J. L., and Scully, J. R., "Origins of Persistent Interaction among Localized Corrosion Sites on Stainless Steel", *Journal of The Electrochemical Society*, Vol. 151, 2004, p. B233–B243